

April, 1996

# Effects of Strong Interaction on the Electromagnetic Dissociation

A. MÜNDEL and G. BAUR

*IKP (Theorie), Forschungszentrum Jülich, D-52425 Jülich, Fed. Rep. Germany.*

## Abstract

We investigate effects of strong interactions on the electromagnetic dissociation of nuclei in heavy ion collisions.

We start from the eikonal approach to the equivalent photon method to describe the electromagnetic contributions to the cross section of peripheral collisions. We summarize some results of this approach and characterize recent experiments in "universal plots".

In the second part of this work, we give a straight forward method to include transitions induced by the strong interactions between the ions. We introduce two different methods to obtain the nuclear transition potential, and study the behavior of the resulting nuclear contributions.

arXiv:nucl-th/9605042v1 31 May 1996

# 1 Introduction

The Coulomb field of a fast moving heavy ion is an intense source of quasi real photons [1, 2, 3]. With raising projectile energy this photon spectrum becomes harder and there exist a variety of applications in nuclear– as well as astrophysics, like the excitation of giant resonances or the Coulomb dissociation of the ions [4].

The advantage of using heavy ions to study this processes are the large cross section, which make the Coulomb dissociation an interesting tool to study even multi–photon resonances [5, 6] or the astrophysical S–factor for reactions like  ${}^7\text{Be}(p, \gamma){}^8\text{B}$  [4]. In the latter case phase-space considerations and the large number of equivalent photons highly favor the Coulomb dissociation compared to the direct measurement of the radiative capture reaction [7, 8].

A powerful but simple tool to describe the Coulomb dissociation of heavy ions is the equivalent photon method [3]. On the other hand this simple approach does not take into account excitations due to the strong interaction. Therefore it is interesting and necessary to study these effects. Using the hydro-dynamical model of Bohr and Tassie for the nuclear transition densities or potentials [9], one can connect the nuclear interaction to the optical potential and the deformation parameter and therefore to the electromagnetic transition matrixelements. This approach allows us to study these contributions in various cases of physical interest.

## 2 Equivalent photon spectrum in a Glauber approach

In the following we consider a situation where a projectile (particle 1) with charge  $Z_1$  excites a target (particle 2) with charge  $Z_2$  from the ground state  $|0\rangle$  to the excited state  $|l, m\rangle$  in a peripheral collision via the exchange of one quasi real photon of energy  $E_\gamma = \hbar\omega$ . The velocity  $\vec{\beta} = \frac{\vec{v}}{c}$  of the projectile is in  $z$  direction and we use  $\gamma = (1 - \beta^2)^{-\frac{1}{2}}$ . The

scattering angle of the projectile is denoted by  $\theta$ . The cross section for this process is given by

$$\frac{d\sigma}{d\Omega} = \sum_F \frac{1}{2I_i + 1} \sum_{M_i M_f} |f(\theta)|^2, \quad (1)$$

where  $I$  is the angular momentum of the nucleus and  $M$  it's magnetic quantum number. The subscripts  $i$  ( $f$ ) denotes the initial (final) state.

In the eikonal approximation [10] the inelastic scattering amplitude  $f(\theta)$  is given by [11]:

$$f(\theta) = \frac{ik}{2\pi\hbar v} \int d^3r d^3r' e^{i\vec{q}\cdot\vec{r}} e^{i\chi(b)} \langle \Phi_f(\vec{r}') | V_{int}(\vec{r}, \vec{r}') | \Phi_i(\vec{r}') \rangle, \quad (2)$$

where  $\vec{q}$  denotes the momentum transfer and  $k$  is the wavenumber of the incoming projectile. We define  $\vec{r}$  to be the separation of the centers of mass of the two nuclei, and  $\vec{r}'$  to be the intrinsic coordinate of the target nucleus.

The Glauber phase  $\chi(b)$  is the sum of a Coulomb and a nuclear part. If we assume the 'sharp cut-off' model for the nuclear part

$$e^{i\chi_N(b)} = \begin{cases} 0 & \text{if } b \leq R = R_1 + R_2 \\ 1 & \text{if } b > R \end{cases}, \quad (3)$$

where  $R_i = 1.2 \text{ fm } A^{1/3}$ , ( $i = 1, 2$ ) is the radius of the  $i$ 'th nucleus, the Coulomb phase is given by

$$\chi_C(b) = 2 \eta \ln(kb). \quad (4)$$

Here  $\eta = \frac{Z_1 Z_2 e^2}{\hbar v}$  is the Sommerfeld parameter.

Using standard methods [3] and defining the reduced electromagnetic transition probabilities  $B(\pi l) = B(\pi l, I_i \rightarrow I_f)$  [12] we can write the cross section in the form

$$\frac{d\sigma}{d\Omega} = \sum_{\pi l} \int \frac{dE_\gamma}{E_\gamma} \sigma_{E_\gamma}^{\pi l}(E_\gamma) \frac{dn^{\pi l}}{d\Omega}. \quad (5)$$

In the above formula  $\sigma_\gamma^{\pi l}(E_\gamma)$  is the photo-nuclear absorption cross section for a given multipolarity [3]

$$\sigma_\gamma^{\pi l}(E_\gamma) = \frac{(2\pi)^3 (l+1)}{l[(2l+1)!!]^2} \sum_F \rho_F(E_\gamma) \kappa^{2l-1} B(\pi l), \quad (6)$$

where  $\rho_F(\omega)$  is the final state density and  $\kappa = \frac{\omega}{c}$ .

Under these assumptions the equivalent photon number per unit solid angle for a given multipolarity  $\frac{dn^{\pi l}}{d\Omega}$  is given by:

$$\frac{dn_C^{\pi l}}{d\Omega} = Z_1^2 \alpha \left( \frac{\omega k}{\gamma v} \right)^2 \frac{l[(2l+1)!!]^2}{(2\pi)^3(l+1)} \sum_m \left| G_{\pi lm} \left( \frac{1}{\beta} \right) \right|^2 |\Omega_m^C(q_T)|^2, \quad (7)$$

Here the transverse momentum transfer  $q_T$  is the only quantity, which depends on the scattering angle. Defining the variables

$$\begin{aligned} x &= \frac{b}{R} \quad ; \quad \xi = \frac{\omega R}{\gamma v}; \\ \Theta_{diff} &= \frac{1}{kR} \quad ; \quad \theta_{gr} = 2\eta\theta_{diff}, \end{aligned} \quad (8)$$

$\Omega_m^C$  can be written as:

$$\Omega_m^C(\theta) = R^2 \int_1^\infty x dx J_m\left(\frac{\theta x}{\theta_{diff}}\right) K_m(\xi x) e^{2i\eta \ln\left(\frac{x}{\theta_{diff}}\right)}. \quad (9)$$

In the case of the classic trajectory of the projectile ( $\eta \rightarrow \infty$ ), one can use the saddle points method to solve the integral in eq. (9)[11]:

$$\Omega_m^{sc}(\theta) = R^2 \frac{y^2}{2\eta} e^{i\tilde{\phi}} K_m(\xi y), \quad (10)$$

where the variables  $y = \frac{\theta_{gr}}{\theta}$  and  $\tilde{\phi} = \frac{1}{2}\pi(m+1) + 2\eta \left( \ln\left(\frac{2\eta}{\theta}\right) - 1 \right)$  where introduced.

Both expressions for  $\Omega_m$  (eqn. 9 and 10) mainly depend on two parameters, the interaction strength  $\eta$  and the adiabaticity parameter  $\xi$ , which is the ratio of transition time to impact time in a grazing collision.

It is interesting to compare  $|2\eta \frac{\Omega_m}{R^2}|^2$  as a function of  $\frac{\theta}{\theta_{gr}}$  for fixed  $\xi$  but different  $\eta$  as shown in the 'universal plots' in figs. (1) and (2). The thick solid line shows the semi classical limit according to eq. (10) while the dashed and dotted lines are the solutions of eq (9) for different values of  $\eta$ . At  $\frac{\theta}{\theta_{gr}} = 1$  the semi classical limit drops to zero while the full solutions extend to higher angles. At small angles the full solution shows diffraction effects, but for a large interval of angles the full solution for sufficiently large  $\eta$  is a fast oscillating function around the semi classical limit (dotted line). Only for small  $\eta$  (dashed line) the full solution differs substantially from the semi classical limit.

For the above reason the semi classical solution for the inelastic scattering amplitude (eq. 2) provides in many relevant cases already a good description of the experimental situation. Fig. (3) classifies some existing experiments in a  $\xi$ - $\eta$ -plot where the experiments well described by the semi classical solution are at large  $\eta$  and small  $\xi$ .

To complete the discussion of the sharp cut-off model we want to give the expression for the total cross section, which is obtained by integrating eq. (5) over the solid angle and using the closure relation for the Bessel functions. One finds:

$$\sigma_{tot} = 2\pi \left(\frac{Ze}{\hbar c}\right)^2 \left(\frac{\omega}{\gamma v}\right)^2 \sum_{\pi l m} \left(\frac{\omega}{c}\right)^{2(l-1)} R^2 \int_1^\infty x dx K_m(\xi x). \quad (11)$$

Notice, that this expression is independent of  $\eta$ .

### 3 The nuclear excitation part

The sharp cut-off model, as it was introduced in the last section, takes nuclear effects into account only in a very simplified way. A more realistic model for the nuclear contributions will influence the inelastic scattering amplitude (eq. 2) in two different ways. First it leads to an additional transition potential in eq. (2) of the form  $\langle \Phi_f(\vec{r}') | V_N | \Phi_i(\vec{r}') \rangle$ , where  $V_N$  is the nuclear potential between the two nuclei. In addition it will change the nuclear phase due to

$$\chi_N(b) = -\frac{1}{\hbar v} \int_{-\infty}^{\infty} V_N(\sqrt{b^2 + z^2}) dz, \quad (12)$$

which, in contrast to the sharp cut-off model, now has a finite real and imaginary part. This leads to a "smoother" cut-off than in the sharp cut-off model and a modification of the Coulomb potential  $V_C$  due to the penetration of the two charge distributions. In the following we will neglect the effect on the Coulomb potential but keep eq. (12), and concentrate on the nuclear induced transitions.

There exist different approaches to obtain the nuclear transition potential (eq. 2)  $\langle \Phi_f(\vec{r}') | V_N | \Phi_i(\vec{r}') \rangle$ . First we want to describe the approach via the transition densities. In this case the nuclear transition potential can be calculated using the folding formalism

[13]:

$$\langle \Phi_f(\vec{r}') | V_N(\vec{r}, \vec{r}') | \Phi_i(\vec{r}') \rangle = \langle t_{NN}(E) \rangle \rho_1(\vec{r} - \vec{r}') \langle l, m | \rho_2(\vec{r}') | 0 \rangle. \quad (13)$$

Here  $\rho_i$ , ( $i = 1, 2$ ) denotes the charge density of the  $i$ 'th nucleus. For the energy dependent  $t_{NN}$ -matrix see ref. [13]. To determine the transition density matrix elements  $\langle l, m | \rho_2(\vec{r}') | 0 \rangle$  we assume the hydro-dynamical model of Bohr and Tassie [9]:

$$\langle l, m | \rho_2(\vec{r}') | 0 \rangle = \frac{\beta_l R_2^{2-l}}{\sqrt{2l+1}} r'^{(l-1)} \frac{d\rho_2(\vec{r}')}{dr'} Y_{lm}^*(\hat{r}'). \quad (14)$$

The deformation parameter  $\beta_l$  is related to the electromagnetic transition matrix elements  $M(E_l, m)$  by:

$$M(E_l, m) = \sqrt{2l+1} \beta_l R_2^{2-l} \int_0^\infty dr r^{2l} \rho_2(r) \quad (15)$$

Under these assumptions the inelastic scattering amplitude (eq. 2) can be written as:

$$f(\theta) = \sum_{\pi l m} \frac{i^{m+1} k}{\hbar v} e^{-im\alpha} M(\pi l, m) \int_0^\infty b db e^{i(\chi_C(b) + \chi_N(b))} J_m(q_T b) \left\{ \Gamma_C^{\pi l m}(b) + \Gamma_N^{\pi l m}(b) \right\}. \quad (16)$$

Since we neglect the corrections of the Coulomb part due to the penetration of the two particle,  $\Gamma_C^{\pi l m}$  is still assumed to be given by:

$$\Gamma_C^{\pi l m} = \frac{Z_1 e}{\gamma} \kappa^l \sqrt{2l+1} G_{\pi l m} \left( \frac{1}{\beta} \right) K_m \left( \frac{\omega b}{\gamma v} \right). \quad (17)$$

For the sake of mathematical simplicity we consider a Gaussian shaped charge distribution for the two nuclei [13] to calculate  $\Gamma_N^{\pi l m}$ :

$$\rho_i(r) = \rho_i(0) e^{-\frac{r^2}{R_{G_i}^2}}; \quad \rho_i(0) = 0.085 f m^{-3} e^{\frac{R_i}{2a_i}}. \quad (18)$$

We have used the notation  $R_{G_i}^2 = 2a_i R_i$ , where  $a_i$  is the diffuseness parameter of the  $i$ 'th nucleus. This choice for the charge distribution allows us to perform most of the calculations in an analytical way.

Under the above assumptions the nuclear phase (eq. 12) is given by [14]

$$\chi_N(b) = \langle t_{NN}(E) \rangle \rho_1(0) \rho_2(0) \left\{ \frac{R_{G_1}^3 R_{G_2}^3}{R_G^2} \right\} e^{-b^2/R_G^2}, \quad (19)$$

where  $R_G^2 = R_{G_1}^2 + R_{G_2}^2$ . To take into account the singularity  $\chi_C(b=0)$  (eq. 4), we modify the Coulomb phase [11]:

$$\chi_C(b) = 2\eta \left\{ \ln(kb) + \frac{1}{2} E_1 \left( \frac{b^2}{R_G^2} \right) \right\}. \quad (20)$$

In the above formula  $E_1$  denotes the exponential integral.

Calculating the nuclear transition density as given in eq. (14) and using eq. (15) we find for  $\Gamma_N^{\pi lm}$  :

$$\begin{aligned} \Gamma_N^{Elm} &= \pi \rho_1(0) \frac{2^{l+2}}{(2l+1)!!} \frac{R_{G_1}^3}{R_G^{2l+3}} \langle t_{NN}(E) \rangle \\ &\quad \int dz r^l e^{i\frac{\omega}{v}z} e^{-\frac{r^2}{R_G^2}} Y_{lm}(\theta_{\hat{r}}, 0), \\ \Gamma_N^{Mlm} &= 0. \end{aligned} \quad (21)$$

The Gauss parameterization for the charge densities is a relatively good approximation for light nuclei, but fail for heavy nuclei. Starting from more realistic densities immediately makes it necessary to solve the folding integral (eq. 13) numerically. To avoid these difficulties one can start from optical potential rather than their corresponding densities. This formalism is described in ref. [15].

In this case the transition potential  $\langle l, m | V_N | 0 \rangle$  is connected to the optical nuclear potential  $V_N(r)$  by

$$\langle l, m | V_N | 0 \rangle = \frac{-1}{\sqrt{2l+1}} \beta_l R_2 \frac{dV(r)}{dr} Y_{lm}^*(\theta, \phi), \quad (22)$$

where for both, the Tassie model and the Bohr Mottelson model [16],  $\beta_l$  is given by

$$\beta_l = \frac{4\pi}{3} \frac{1}{Z_2 R_2^l} \sqrt{B(El)}. \quad (23)$$

Using eqn. (22, 23 and 16) we find for  $\Gamma_N^{Elm}$  :

$$\Gamma_N^{Elm} = \frac{-4\pi}{3Z_2 R_2^{l-1}} \int dz e^{i\frac{\omega}{v}z} \frac{dV}{dr} Y_{lm}(\theta_{\hat{r}}, 0). \quad (24)$$

First we want to assume a Woods–Saxon parameterization for the nuclear potential  $V_N = U(r) + iW(r)$  with:

$$U(r) = -U_0 \left( e^{\frac{r-R_U}{aU}} + 1 \right)^{-1}; \quad W(r) = -W_0 \left( e^{\frac{r-R_W}{aW}} + 1 \right)^{-1}. \quad (25)$$

In fig (4) we show the results with the above formalism for the Coulomb dissociation of  ${}^8B$ , an experiment recently made, to determine the astrophysical S-factor of the  ${}^7B(p, \gamma){}^8B$  reaction [17]. The figure shows the cross section for a  ${}^{208}Pb$  target and a  $46MeV/nucleon$   ${}^8B$  beam. The excitation energy is assumed to be  $0.6MeV$ . The solid line shows the total cross section ( $E1 + E2$ ), the dashed line the sum of the Coulomb and nuclear contribution for  $l = 2$  ( $E2_{C+N}$ ), and the dotted line gives the  $E2_N$  contribution only. We used  $B(E1) = 0.462b$  and  $B(E2) = 0,148b^2$ . For the Woods-Saxon potential we assumed the following parameters,

$$\begin{aligned} U_0 &= 40MeV \quad ; \quad W_0 = 45MeV \quad ; \\ R_U &= R_W = 10.2fm \quad ; \quad a_U = a_W = 0.6fm, \end{aligned} \quad (26)$$

Fig (4) shows, that the dissociation of  ${}^8B$  via nuclear excitation plays only a minor role in this experiments. The total cross section can be well described with the simple semi-classical model (eqn. 10 and 7).

A more schematic model for the optical potential  $V_N = U_N + iW_N$  is given by the "ramp" potential,

$$U(r) = \begin{cases} -U_0 & \text{if } r < R_U^- \\ -\frac{U_0}{\Delta_U}(R_U^+ - r) & \text{if } R_U^- \leq r \leq R_U^+ \\ 0 & \text{if } r > R_U^+ \end{cases}, \quad (27)$$

where  $R_U^\pm = R_U \pm \frac{\Delta_U}{2}$ . The imaginary part  $W_N$  is given in a similar way.

Fig. (5) compares the nuclear phase  $|e^{i\chi_N(b)}|^2$  and  $|\Gamma_N^{lm}(b)|^2$  for Woods-Saxon (solid line) and the "ramp" potential (dashed line). The functions were calculated at  $\theta = 2.0^\circ$ , for  $l = 1$ ,  $m = 0$ , and are plotted as a function of  $b/R$ . For the Woods-Saxon potential we used  $U_0 = 28MeV$ ,  $W_0 = 30MeV$ ,  $R_U = R_W = R = 10.2fm$ , and  $a_U = a_W = 0.6$  and for the "ramp" potential  $U_0 = W_0 = 30MeV$ ,  $R_U = R_W = 9.5fm$ , and  $\Delta_U = \Delta_W = 6fm$ . One finds, that for an adequate choice of parameters both models give nearly the same results.

Because the product  $|e^{i\chi_N(b)}\Gamma_N^{lm}(b)|$  is a good measure for the nuclear transition strength, we want to deduce some basic features of this quantity. The magnitude of the real part

$U_0$  is directly proportional to the magnitude of  $|\Gamma_N^{lm}(b)|$ , while the imaginary part  $W_N$  mainly influences the shape of  $|e^{i\chi_N(b)}|^2$ . Namely for decreasing  $W_0$  the contributions for  $b < R - \Delta_W$  in eq. (16) becomes important. This leads to an increasing nuclear contribution, while the oscillations of the Coulomb contribution around the semi classical limit (figs. 1 and 2) decrease. For the radii a choice like  $R_U > R_W$  will lead to a larger overlap in fig. (5) and therefore to a larger value for  $|e^{i\chi_N(b)}\Gamma_N^{lm}(b)|$ .

This shows, that the magnitude of the nuclear contribution can vary over a wide range (one order of magnitude) if one uses different but still physical meaningful sets of parameters for the optical potential.

For sufficiently large  $W_0$  and small  $\Delta$  one can deduce a very simple expression for the "ramp" model. For simplicity we assume  $R_U = R_W = R$  and  $\Delta_U = \Delta_W = \Delta$ . The nuclear phase is then approximately given by

$$e^{i\chi_N(b)} = \begin{cases} 0 & \text{if } b < R_U^- \\ \frac{b-R^-}{\Delta} & \text{if } R_U^- \leq b \leq R_U^+ \\ 1 & \text{if } b > R_U^+ \end{cases}, \quad (28)$$

Using this approximations, we find for  $e^{i\chi(b)}\Gamma_N^{Elm}(b)$ :

$$e^{i\chi_N(b)}\Gamma_N^{Elm}(b) = \frac{4\pi}{3Z_2R_2^{l+1}} \frac{b-R^-}{\Delta^2} (U_0 + iW_0) Y_{lm}\left(\frac{\pi}{2}, 0\right) \frac{2v}{\omega} \sin\left(\frac{\omega z_{max}}{v}\right), \quad (29)$$

for  $R_U^- \leq b \leq R_U^+$  and zero otherwise. In eq. (29) we used  $Y_{lm}(\theta_{\hat{r}}, 0) \approx Y_{lm}(\frac{\pi}{2}, 0)$  and we have defined  $z_{max} = \sqrt{R^+{}^2 - b^2}$ .

Expanding the sinus for small arguments and introducing the variables  $D = (R_1 - R_2)/R$ ,  $x = b/R$ , and  $\delta = \Delta/R$  one can write eq. (29)

$$e^{i\chi_N(x)}\Gamma_N^{Elm}(x) = \frac{8\pi}{3Z_2} \frac{2^l}{R^{l-2}} \frac{U_0 + iW_0}{(1-D)^{l+1}} \frac{1}{\delta} (x-1+\delta) \sqrt{\left(1+\frac{\delta}{2}\right)^2 - x^2}. \quad (30)$$

This expression is proportional  $\frac{1}{\sqrt{\delta}}$  for  $\delta \rightarrow 0$ . The integral over impact parameter (eq. 16) ranges from  $R^-$  to  $R^+$  and is therefore proportional to  $R^2\delta$ . This shows, that the nuclear contribution (eq. 16) vanish in the limit of the sharp cut-off model.

To see the influence of the parameters  $\delta$  and  $D$  Fig. (6) shows  $|f_N^{E22}(\theta)|^2$  obtained from eq. (29) as a function of  $\theta/\theta_{gr}$  for different values of  $\delta$  (solid line  $\delta = 0.5$ , dashed line  $\delta = 0.1$  and dotted line  $\delta = 0.02$ ). We used  $D = 0.5$ ,  $\xi = 0.1$  and  $\eta = 9$ . Fig (7) shows the same for fixed  $\delta = 0.5$  but varying  $D$  (solid line  $D = 0.5$ , dashed line  $D = 0.3$  and dotted line  $D = 0$ ).

We want to stress, that  $\Gamma_N^{Elm}$  is nearly independent from the excitation energy  $\omega$ , while  $\Gamma_C^{Elm}$  decreases with increasing excitation energy due to the behavior of  $K_m\left(\frac{\omega b}{\gamma v}\right)$  (eq. 17).

## 4 Conclusions

Using so called "universal plots", it is possible, to characterize the Coulomb contributions to peripheral heavy ion collisions. The relevant parameters are the interaction strength  $\eta$ , the adiabaticity parameter  $\xi$ , and  $\theta/\theta_{gr}$ . It turns out, that for many experiments a semi-classical approach to the equivalent photon method is already a sufficiently good description of the data.

In the second part, we could include the nuclear excitation in a straight forward way. We used the folding formalism and the optical potential model, to determine the nuclear transition potential. The introduction of the simplified "ramp" model makes it possible to clarify the role of the parameters of the used optical potentials. Even though the nuclear contribution may vary over a wide range for different potential parameterizations, it turns out, that in many relevant cases, the nuclear contributions are clearly dominated by the Coulomb effects.

## References

- [1] C.F. Weizäcker, *Z. Phys.* **88** (1934) 612.
- [2] E.J. Williams, *Phys. Rev.* **45** (1934) 729.
- [3] C.A. Bertulani and G. Baur, *Phys. Rep.* **163** (1988) 299.
- [4] G. Baur and H. Rebel, *J. Phys. G* **20** (1994) 1.
- [5] T. Aumann, C.A. Bertulani and K. Sümmerer *Phys. Rev. C* **51** (1995) 416.
- [6] H. Emling *Prog. Part. Nucl. Phys.* **33** (1994) 729.
- [7] S. Typel and G. Baur, *Phys. Rev. C* **50** (1994) 2104.
- [8] H. Esbensen and G.F.Bertsch, *Phys. Lett. B* **359** (1995) 13.
- [9] L.J. Tassie, *Austral. J. Phys.* **9**(1956)407.
- [10] R.J. Glauber, *Lectures in theoretical Physics I* (Interscience Publishers, Inc., New York 1959).
- [11] C.A. Bertulani and A.M. Nathan *Nucl. Phys. A* **554** (1993) 158.
- [12] K. Alder and A. Winther, *Electromagnetic Excitation* (North Holland, Amsterdam, 1965).
- [13] A.N.F. Aleixo and C.A. Berulani *Nucl. Phys. A* **528** (1991) 436.
- [14] P.J. Karol, *Phys. Rev. C* **11** (1975) 1203.
- [15] G.R. Satchler *Nucl. Phys. A* **472** (1987) 215.
- [16] A.Bohr and B.R. Mottelson, *Nuclear Structure*, vol. 2 (Benjamin, New York, 1971)
- [17] T.Motobayashi et al., *Phys. Rev. Lett.* **70** (1994) 2680.

# Figures

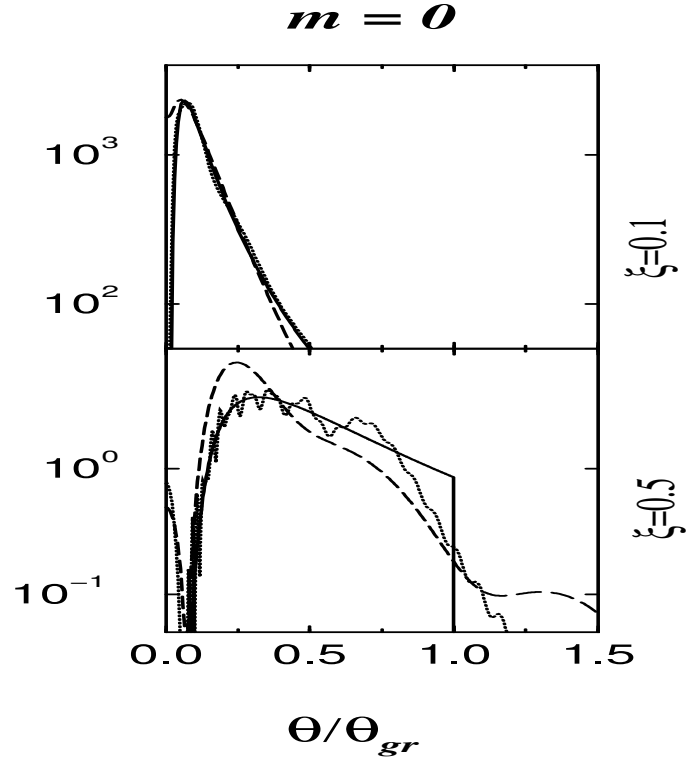


Figure 1:  $|2\eta\frac{\Omega_0}{R^2}|^2$  for  $\xi = 0.5$ ,  $\eta = 20$  (dashed) and  $\eta = 2$  (thin) upper picture and for  $\xi = 0.1$ ,  $\eta = 3$  (dashed) and  $\eta = 1.2$  (thin) lower one. The thick line shows result for the semi classical expression (eq. 10).

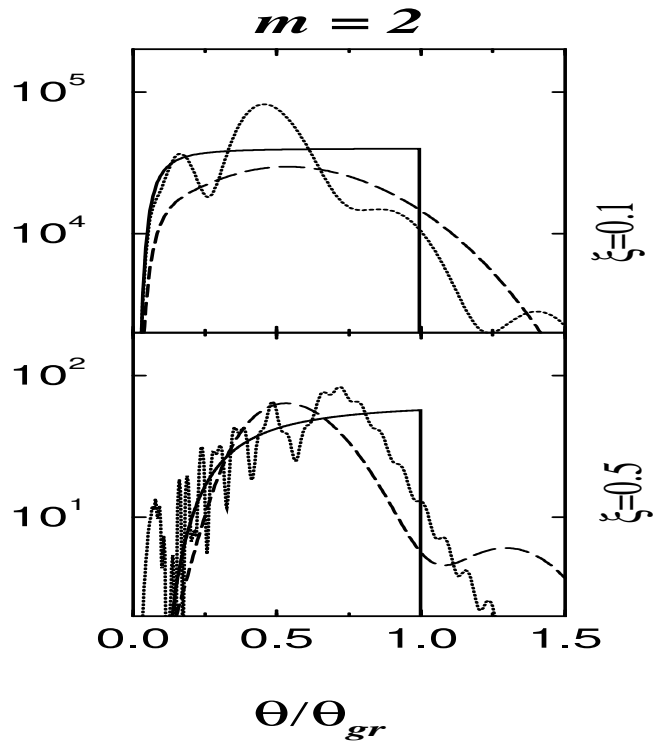


Figure 2: Same as fig. (1) but for  $m = 2$

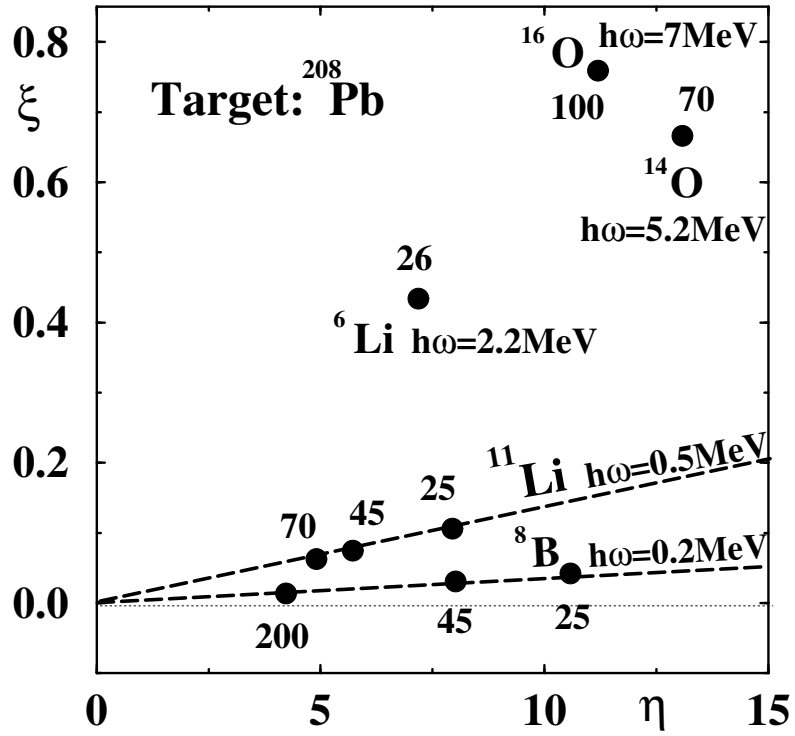


Figure 3: Some experiments characterized in a  $\xi$ - $\eta$ -plot.

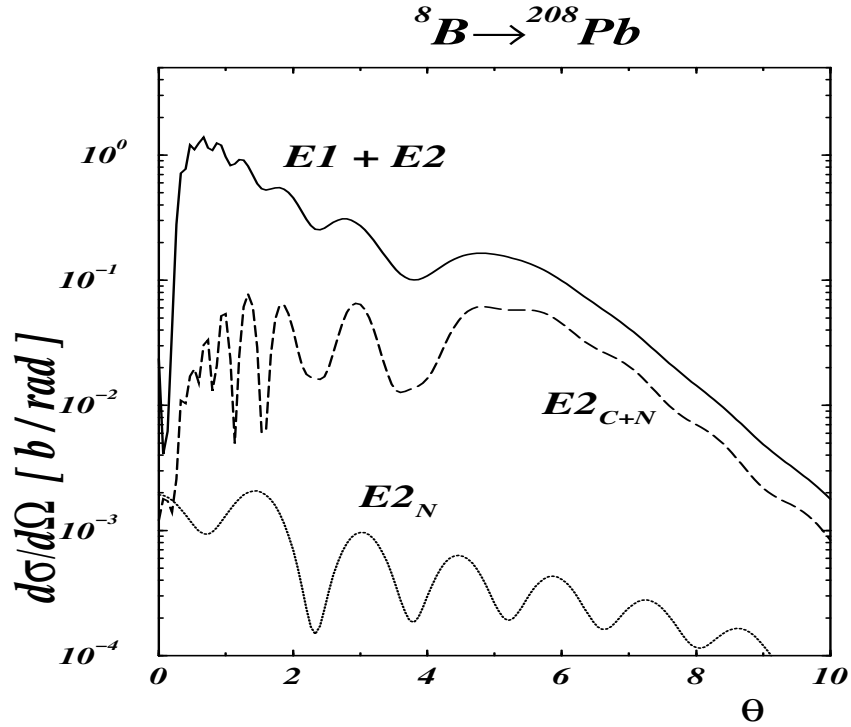


Figure 4: Cross section for the Coulomb dissociation of  $46\text{MeV/nucleon } {}^8B$  beam on a  ${}^{208}Pb$  target. The solid line shows the total cross section, while the dashed gives the  $E2_{C+N}$ , and the lower line only the  $E2_N$  contribution

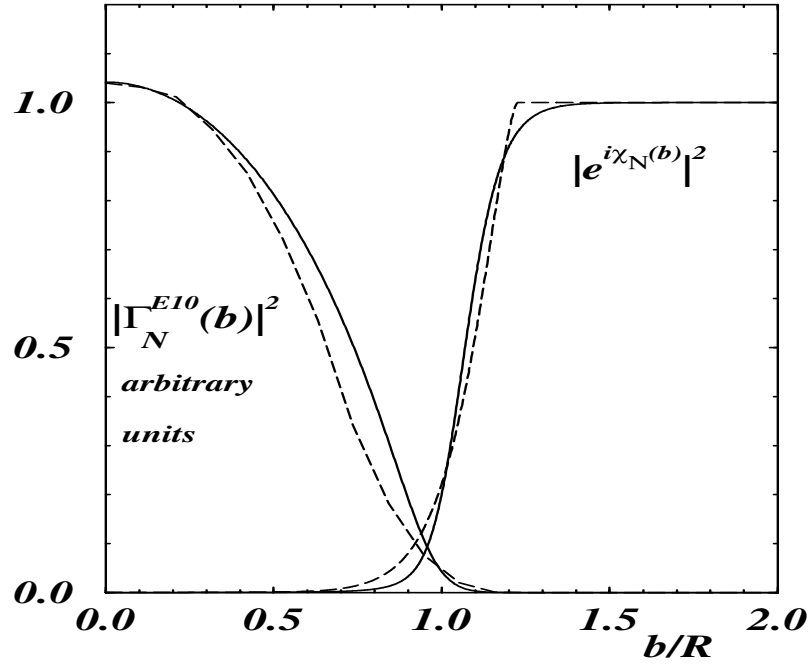


Figure 5:  $|\Gamma_N^{E10}(b)|^2$  (left hand side) and  $|e^{i\chi_N(b)}|^2$  (right hand side) as a function of  $\frac{b}{R}$ . The solid and the dashed line belong to the Woods-Saxon model and the simplified model respectively.

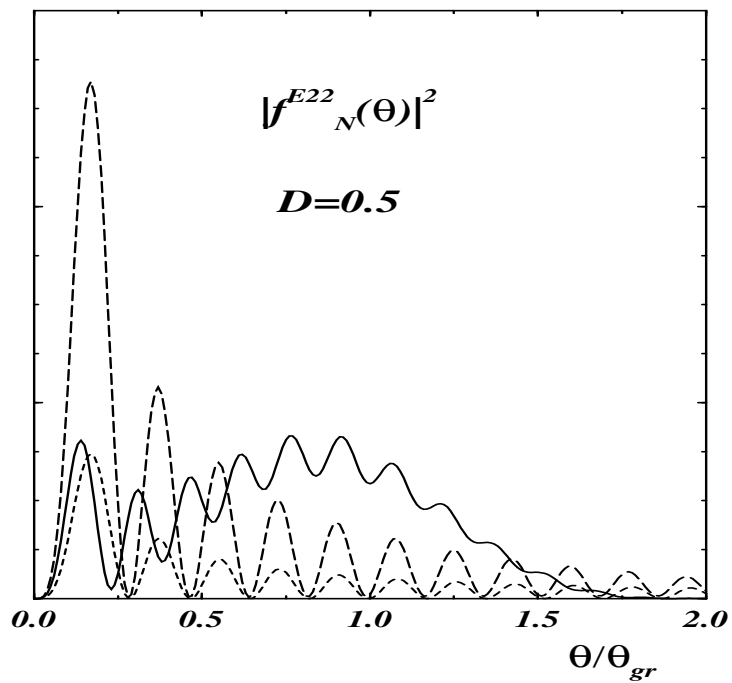


Figure 6:  $|f_N^{E22}(\theta)|^2$  as a function of  $\theta/\theta_{gr}$  for different values of  $\delta$  (solid line  $\delta = 0.5$ , dashed line  $\delta = 0.1$  and dotted line  $\delta = 0.02$ )

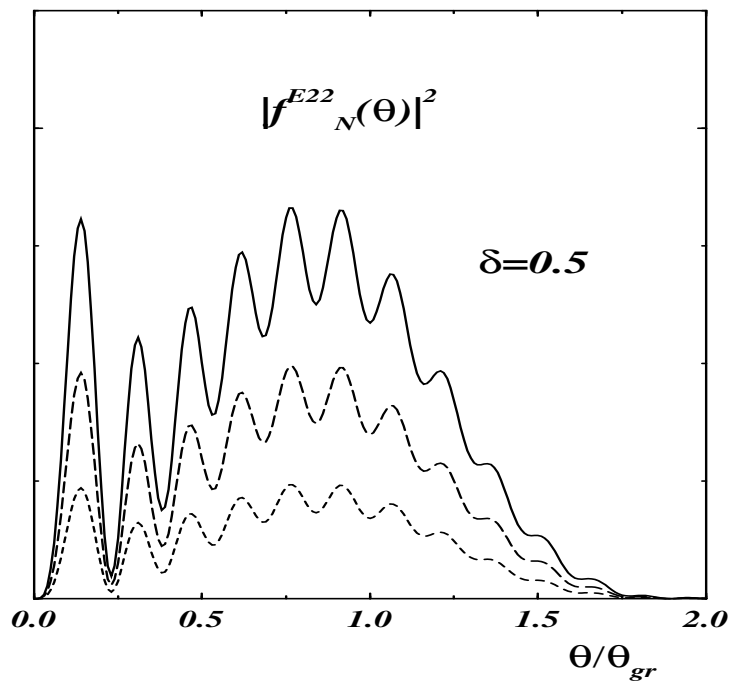


Figure 7:  $|f_N^{E22}(\theta)|^2$  as a function of  $\theta/\theta_{gr}$  for different values of  $D$  (solid line  $D = 0.5$ , dashed line  $D = 0.3$  and dotted line  $D = 0$ ).